Temperature Dependence of Gel Properties of Two-Component Physical Gels

Ching-Feng Mao

Department of Chemical Engineering, Southern Taiwan University of Technology, Tainan, Taiwan, Republic of China

Received 6 September 2005; accepted November 2006
DOI 10.1002/app.24767
Published online in Wiley InterScience (www.interscience.wiley.com).

ABSTRACT: The cascade model for mixed gels developed by the author in a previous work is extended to describe the temperature-dependent gel properties. The equilibrium constant of the association between component polymers is assumed to depend on temperature via a van't Hoff-type equation. The temperature variation of the network structure and gel modulus is presented and discussed at different parameters such as enthalpy change per crosslink $\Delta H°$, entropy change per crosslink $\Delta S°$, functionality ratio s, and concentration ratio r. It is demonstrated that the model agrees reasonably well with the experimental data obtained from the rheological gelling for galactomannan/xanthan and glucomannan/xanthan mixed gels. However, the resulting model parameters are not consistent with those obtained from the concentration dependence study. A further investigation on the calorimetric thermogram of the glucomannan/xanthan mixed gel reveals that the gelling process involves an association reaction followed by a structural rearrangement, which is beyond the scope of this work. Finally, the cascade model is shown to be consistent with the Eldridge–Ferry equation. It is also demonstrated that the sol–gel behavior of the galactomannan/xanthan mixed gel follows the Eldridge–Ferry relationship, but the calculated melting enthalpy is composition-dependent, contrary to the assumption made in the cascade model. This discrepancy is due to the self-association of xanthan when xanthan is present in excess amounts. J Appl Polym Sci 102: 663–673, 2006

Key words: cascade model; gels; modulus; sol–gel transition

INTRODUCTION

The interaction between two different polymers in solutions may result in an enhancement in rheological properties or gel strengths. Because of its importance in practice, multicomponent polymer gels have attracted the interest of many researchers for the last two decades. For example, in the food industry, it is well-known that galactomannan can interact with xanthan in solutions to form a gel.[1] It has been proposed that the gel network is formed via the synergistic binding between xanthan and the galactose-free mannan segment.[2] Another example relating to this problem is the increase in gel strength of gelatin gels when adding small amounts of gellan.[3] The gel network has been suggested to be composed of a continuous gellan phase and a discontinuous gelatin filler.[4] In medical science, a combination of polymers is often used in the formulation of drug delivery systems to improve gelling properties. For example, a Pluronic-based solution, used as a gelling vehicle for ophthalmic drugs, shows a significant increase in viscosity when alginate is added.[5] An aqueous solution containing polyacrylic acid and hydroxypropyl methylcellulose, which is formulated to reduce the amount of highly acidic polyacrylic acid, undergoes a sol–gel phase transition under physiological pH conditions.[6] Despite the success in tailoring the rheological properties of drug delivery systems, the interaction between different polymers in these systems is still poorly understood. An understanding of the interaction pattern and its relationship to the gelling properties is therefore of importance both in engineering practice and scientific research.

The simplest scheme for the interaction between component polymers in a two-component physical gel involves only the noncovalent association of segments of the two polymers. The gel network generated in this way is called a coupled network.[7] In our previous article,[8] we discussed the gel modulus and the gel point of a coupled network. We assumed that the interaction between the two components follows a pairwise reaction at equilibrium and the network structure is described by a cascade model.[9] The concentration dependence of gel modulus was shown to be a function of functionalities (number of functional groups in a polymer chain), the equilibrium constant of the pairwise reaction, and the front factor (a measure of deviation from ideal rubber elasticity). We also showed that the concentration ratio and the functionality ratio of the two components play a key role in determining the gel modulus. Therefore, a mixed gel system can be characterized by the variation of the gel

Correspondence to: C.-F. Mao (cfmao@mail.stut.edu.tw).

modulus and the gel point with respect to the concentration ratio, and it was demonstrated that the model parameters could be obtained from the experimental data of gel moduli or gel points measured at a series of concentration ratios. These parameters are helpful in predicting the gelling properties of a two-component polymer gel, and in throwing light on the nature of the interaction pattern and the resulting network structure.

In addition to the aforementioned concentration dependence of gel properties, the temperature dependence of gel properties is also of great importance for physical gels. Physical gels are usually thermoreversible, since the crosslinks are formed through weak interactions, where the binding energy is of the order of thermal energy. Therefore, on heating, thermoreversible gels undergo a sol–gel transition. For single-component thermoreversible gels, the concentration dependence of the melting temperature has been modeled by the Eldridge–Ferry equation.[10] The modulus of physical gels also varies significantly as temperature changes. In some recent publications,[11,12] the temperature dependence of gel modulus of single-component physical gels was analyzed based on a cascade model, and the nature of network junctions was discussed in terms of the parameters of the model.

The aim of this study is to extend the cascade analysis of coupled two-component physical gels to include the effect of temperature. First, the temperature dependence of the network structure and gel modulus is examined by assuming that the temperature dependence of the equilibrium constant follows a van't Hoff-type relation. Second, the applicability of the Eldridge–Ferry equation to two-component thermoreversible gel systems is justified, and its relationship with the cascade model is discussed. Finally, experimental data, including the temperature dependence of gel modulus and sol–gel phase diagrams, are used to demonstrate the validity of this temperature dependence approach.

CASCADE MODEL

In our previous study, the cascade model for a coupled two-component polymer gel was developed based on a simple interaction scheme[8]: The junction zones of gel networks are formed via the interaction between the crosslinking sites of two different polymers:

$$\mathrm{A} + \mathrm{B} \leftrightarrow \mathrm{AB} \tag{1}$$

The two polymers of molecular weights M_A and M_B carrying functionalities f_A and f_B are mixed with a concentration ratio r ($= C_B/C_A$). Thus, the conversions of the two kinds of crosslinking sites α_A and α_B can be obtained from the equilibrium equation:

$$K = \frac{\alpha_A}{(C_B / M_B) f_B (1 - \alpha_A)(1 - \alpha_B)} \tag{2}$$

where K is the equilibrium constant. If one assumes that the temperature dependence of the equilibrium constant obeys the van't Hoff-type relation, K can be written as a function of temperature in terms of the enthalpy change and entropy change per crosslink.[13]

$$K = \exp\left(\frac{\Delta S^\circ}{R} - \frac{\Delta H^\circ}{RT}\right) \tag{3}$$

Equations (2) and (3) together determine the temperature dependence of α_A and α_B.

The structure of gel networks in the cascade theory is modeled by a branching process, which is characterized by an extinction probability, representing the probability of a link becoming extinct. For a two-component polymer gel, there are two extinction probabilities, v_A and v_B, and the solution of them is coupled:

$$v_A = (1 - \alpha_A + \alpha_A v_B)^{f_A - 1} \tag{4a}$$

$$v_B = (1 - \alpha_B + \alpha_B v_A)^{f_B - 1} \tag{4b}$$

Since α_A and α_B are temperature dependent, eq. (4) allows the calculation of v_A and v_B as a function of temperature.

In the cascade model, the elasticity of polymer gels is proportional to the number of elastically active network chains (EANCs) emanating from a repeating unit (a polymer chain for physical gels).[14,15] Once the conversions and extinction probabilities are determined, the number of EANCs for the two polymers N_{eA} and N_{eB} can be calculated by the following equations:

$$N_{cA} = \frac{1}{2} f_A \alpha_A (1 - v_B)[1 - v_A - (f_A - 1)\alpha_A v_A (1 - v_B) / (1 - \alpha_A + \alpha_A v_B)] \tag{5a}$$

$$N_{cB} = \frac{1}{2} f_B \alpha_B (1 - v_A)[1 - v_B - (f_B - 1)\alpha_B v_B)(1 - v_A) / (1 - \alpha_B + \alpha_B v_A)] \tag{5b}$$

Consequently, N_{eA} and N_{eB} are also a function of temperature. It is noted that for chemical gels, the number of EANCs is fixed and considered to be temperature-independent.

TEMPERATURE DEPENDENCE OF CONVERSION, EXTINCTION PROBABILITY, AND NUMBER OF EANCS

The temperature dependence of the network structure of a physical gel can be calculated from eqs. (2)–(5).

Equation (3) reveals that ΔH° and ΔS° are key parameters in determining the temperature effect. Thus, knowledge of the range of ΔH° and ΔS° is essential in applying eq. (3).

The value of ΔH° in the self-association reaction for a single-component physical gel is often obtained from the sol–gel phase diagram, using the Eldridge–Ferry plot as the melting enthalpy per crosslink. The reported melting enthalpies vary over a wide range, from a large value of 1300 kJ/mol for agarose gels[16] to a value less than 10 kJ/mol for polystyrene gels and nitrocellulose gels.[17,18]

In contrast to the abundant literature on the enthalpy for physical crosslinks, the entropy in a crosslink is less reported. One way to estimate the entropy is to fit the gel modulus curve in a temperature sweep, using the cascade model. For example, ΔH° and ΔS° for locust bean gum gels have been estimated to be -99.6 kJ/mol and -0.201 kJ/(mol K), respectively, from a rheological meltdown curve.[11] The minus sign of ΔS° indicates an entropic cost as a consequence of degrees of freedom of motion lost when crosslinking occurs. This phenomenon is known as the enthalpy–entropy compensation.[19] It is noted that these values obey the linear correlation between enthalpy and entropy observed for the associations of low-molecular-weight molecules in solution[19]:

$$\frac{\Delta H^\circ}{300\Delta S^\circ} \approx 1.59 \qquad (6)$$

In this section, the temperature variation of the network structure is discussed based on this correlation, and cases with the enthalpy–entropy ratio other than 1.59 are also examined.

Figure 1 shows the temperature dependence of conversion, extinction probability, and the number of EANCs for two-component physical gels under different dimensionless enthalpy–entropy ratios. All the calculations are performed based on a total polymer concentration of 10 g/L, a functionality of 50 and a molecular weight of 2×10^6 for both polymers, and the concentration ratio and functionality ratio are set to be unity (curves of both polymers thus overlap). To make N_{eA} and N_{eB} comparable, the value of N_e is normalized by f. It can be seen that the conversion decreases with increasing temperature and decreasing enthalpy–entropy ratio because of a decrease in equilibrium constant. Extinction probability, on the other hand, is negligibly small, but as temperature increases near the sol–gel transition temperature (curves at lower enthalpy–entropy ratios), it becomes significant and reaches a value of unity above the transition temperature. Consequently, though the temperature dependence of the normalized N_e generally follows the temperature dependence of the conversion curve, it becomes zero above the transition temperature, regardless of the value of conversions, because of the $(1 - v)$ term in eq. (5).

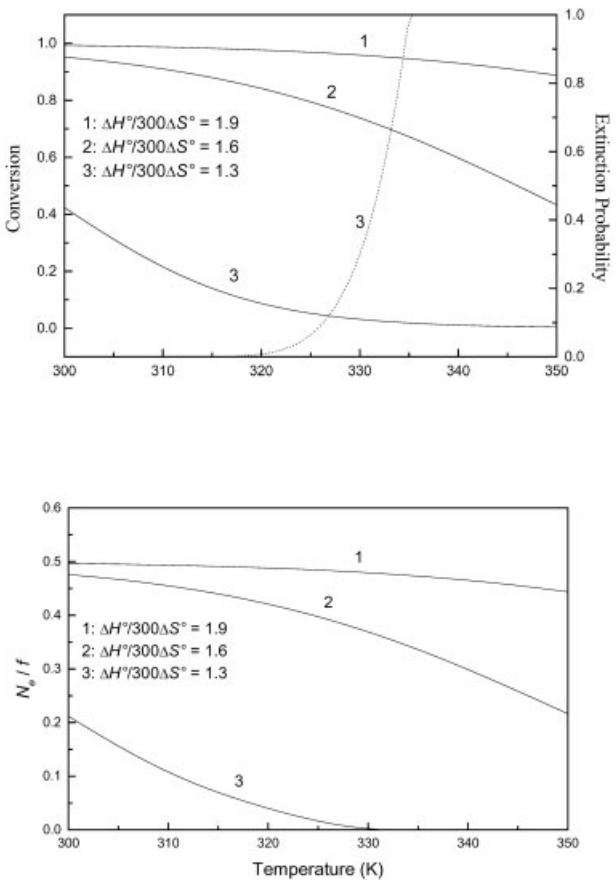

Figure 1 Conversion, extinction probability, and N_e/f as a function of temperature at different dimensionless enthalpy–entropy ratios with $f_A = f_B = 50$, $r = 1$, and $\Delta H^\circ/300R = -40$. Upper plots, conversion (solid curves) and extinction probability (dotted curves); lower plots, N_e/f.

Our previous study has shown that the network structure of a two-component polymer gel is strongly dependent on the functionality ratio s $(= f_B/f_A)$ and the concentration ratio r $(= C_B/C_A)$. It is thus of interest to examine the temperature-dependence curves at different functionality ratios and concentration ratios. Figure 2 demonstrates the effect of functionality ratio on the temperature dependence of conversion, extinction probability, and the number of EANCs at fixed ΔH° and ΔS°. In the case where functionality ratios are other than unity, the temperature dependence curves are split into two separate curves for polymer A and B, respectively. When the functionality ratio is higher than unity, there is a higher opportunity for functional groups A to react; thus, the curves for α_A and N_{eA}/f_A are higher than those for α_B and N_{eB}/f_B, and vice versa. It is also noted that, when $s = 1$ or 10, the extinction probabilities are essentially zero, whereas when $s = 0.1$, they become significant because of the relatively

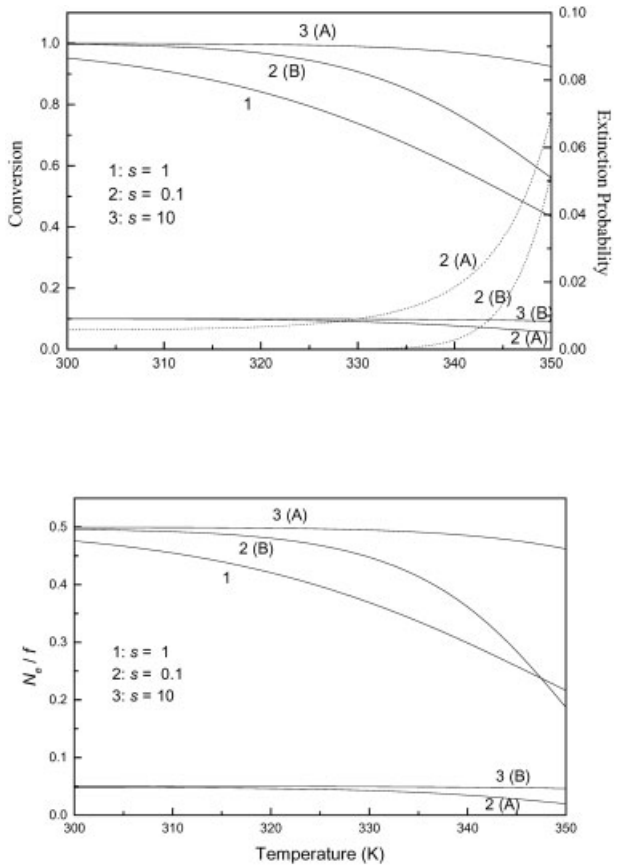

Figure 2 Conversion, extinction probability, and N_e/f as a function of temperature at different functionality ratios with $f_A = 50$, $r = 1$, $\Delta H°/300R = -40$, and $\Delta H°/300\Delta S° = 1.6$. Upper plot, conversion (solid curves) and extinction probability (dotted curves); lower plot, N_e/f.

low value of f_B. The increase in extinction probabilities at $s = 0.1$ causes a more rapid drop in N_e/f as temperature increases.

Figure 3 shows the effect of concentration ratio on the temperature dependence curves. Similar to the effect of functionality ratio, the deviation of concentration ratios from unity causes a splitting of the temperature dependence curves into two. Similarly, when the concentration ratio is higher than unity, there is a higher opportunity for functional groups A to react, leading to higher values of α_A and N_{eA}/f_A. The curves for $r < 1$ are not shown because they overlap with those for $r > 1$. For example, the curves for $r = 0.1$ are identical with those for $r = 10$, but the labels for A and B are switched. It is noted that in Figure 3, the value of extinction probabilities is zero or very small; thus, the temperature dependence of N_e/f generally follows the trend of α.

TEMPERATURE DEPENDENCE OF GEL MODULUS

One of the characteristics of a gel is its elasticity, which can be measured as gel modulus using a rheometer. In the cascade model, the gel modulus G for a two-component polymer gel can be expressed in terms of the algebraic sum of the number of elastic active chains for each individual component[8]:

$$G = aRT[N_{eA}(C_A/M_A) + N_{eB}(C_B/M_B)] \qquad (7)$$

where a is the front factor, an empirical parameter representing the deviations from the ideal rubber elasticity. For an ideal rubber, eq. (7) implies that gel modulus is proportional to temperature because N_e is temperature-independent. On the other hand, for physical gels, N_e varies with temperature such that gel modulus is a complex function of temperature. Equation (7) also implies that gel modulus vanishes when both values of N_e become zero. This occurs as temperature increases beyond the sol–gel transition temperature for a thermoreversible gel. The lowest temperature of zero modulus denotes the melting point (or the gel point) of a thermoreversible gel (practically the melting point is determined as the intersection of storage and loss moduli[20]). The effect of $\Delta H°$, $\Delta S°$, func-

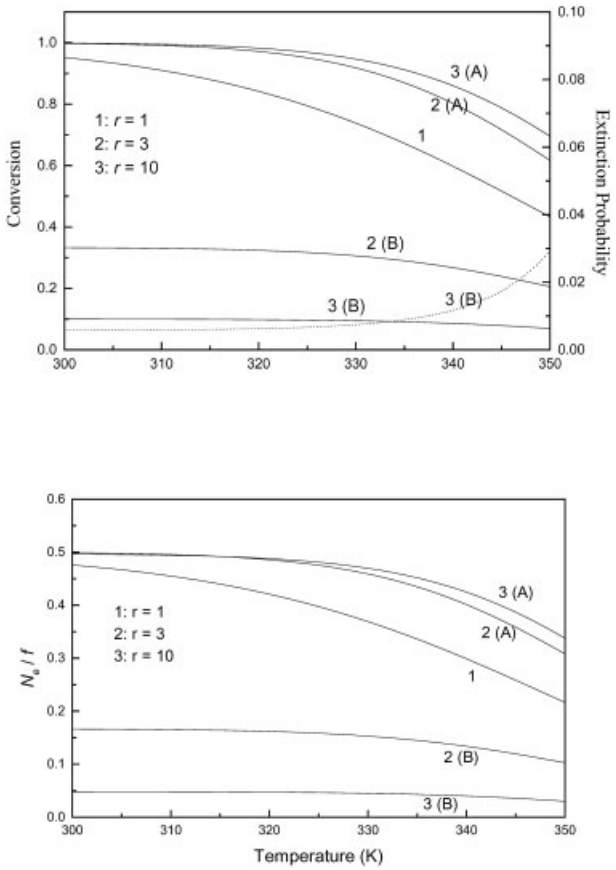

Figure 3 Conversion, extinction probability, and N_e/f as a function of temperature at different concentration ratios with $f_A = f_B = 50$, $\Delta H°/300R = -40$, and $\Delta H°/300\Delta S° = 1.6$. Upper plot, conversion (solid curves) and extinction probability (dotted curves); lower plot, N_e/f.

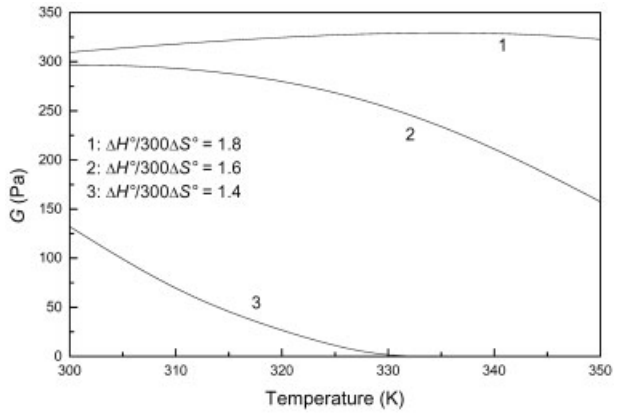

Figure 4 Temperature dependence of G at different dimensionless enthalpy–entropy ratios with $f_A = f_B = 50$, $r = 1$, and $\Delta H°/300R = -40$.

tionality ratios, and concentration ratios on the temperature dependence of gel modulus is examined, and the applicability of eq. (7) to experimental rheological data is discussed here.

Figure 4 shows the temperature dependence of gel modulus at different dimensionless enthalpy–entropy ratios. All the parameters are identical to those used in Figure 1. In comparison with Figure 1, it can be seen that the G versus T curves follow the temperature dependence of N_e/f, as expected in eq. (7). However, when N_e is weakly dependent on temperature (curve 1 at low temperatures), the RT term in eq. (7) dominates, showing an ideal rubber behavior (i.e., gel modulus is proportional to temperature). In this case, the gel does not experience a sol–gel transition within the temperature range studied, showing the characteristics of a thermoirreversible gel. At the other extreme (curve 3), the thermal variation of N_e determines the temperature dependence of G and a melting point can be observed ($G = 0$), showing the characteristics of a thermoreversible gel. Between these two extremes, a maximum value of gel moduli can be found in the G versus T curve. It should be noted that in some cases, although the cascade model predicts the existence of a melting point at high temperatures, practically the polymer may pyrolyze before the temperature reaches the melting point.

For a two-component polymer gel, its gel properties can be characterized by the concentration ratio dependence. Figure 5 illustrates the effect of concentration ratio on G versus T curves at different functionality ratios. Unless otherwise specified, the parameters are identical to those used in Figures 2 and 3. It can be seen that when the functionalities for both polymers are identical [Fig. 5(a)], the gel modulus has the highest value at $r = 1$ and the G versus T curves with reciprocal r values overlap each other. On the other hand, when functionality ratios are other than unity, the largest value of moduli may not occur at $r = 1$ and the temperature dependence of G behaves differently at different concentration ratios. For example, at $s = 0.1$ [Fig. 5(b)], a high r value gives rise to high modulus at low temperatures, but the decrease in modulus as temperature increases occurs earlier and faster. This feature suggests that estimating the functionality ratio of a two-component physical gel can be achieved by examining the experimental G versus T curves at several r values.

Next, the experimental G versus T data for two-component physical gels are investigated to demonstrate the applicability of the cascade model. The galactomannan/xanthan mixed gel is one of the most extensively studied two-component systems because of the distinct synergistic interaction between the two polysaccharides.[21,22] It is known that the junction point of its gel network is formed via the interaction of one segment of unsubstituted mannan with another segment of xanthan.[21,23] This interaction model satisfies the assumption of eq. (1). Goycoolea et al.[24] have measured the concentration dependence and temper-

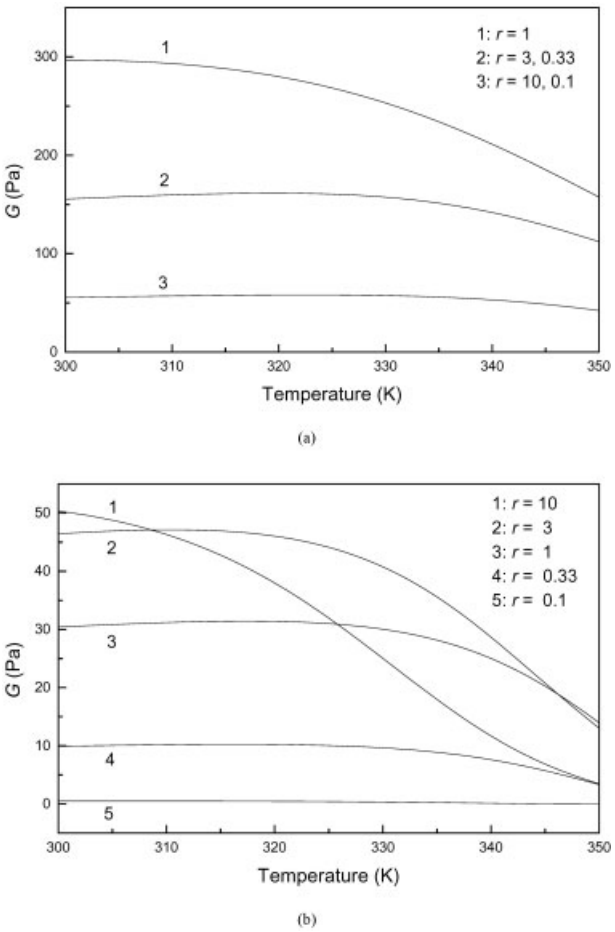

Figure 5 Temperature dependence of G at different concentration ratios with $a = 1$, $f_A = 50$, $\Delta H°/300R = -40$, and $\Delta H°/300\Delta S° = 1.6$. (a) $s = 1$; (b) $s = 0.1$.

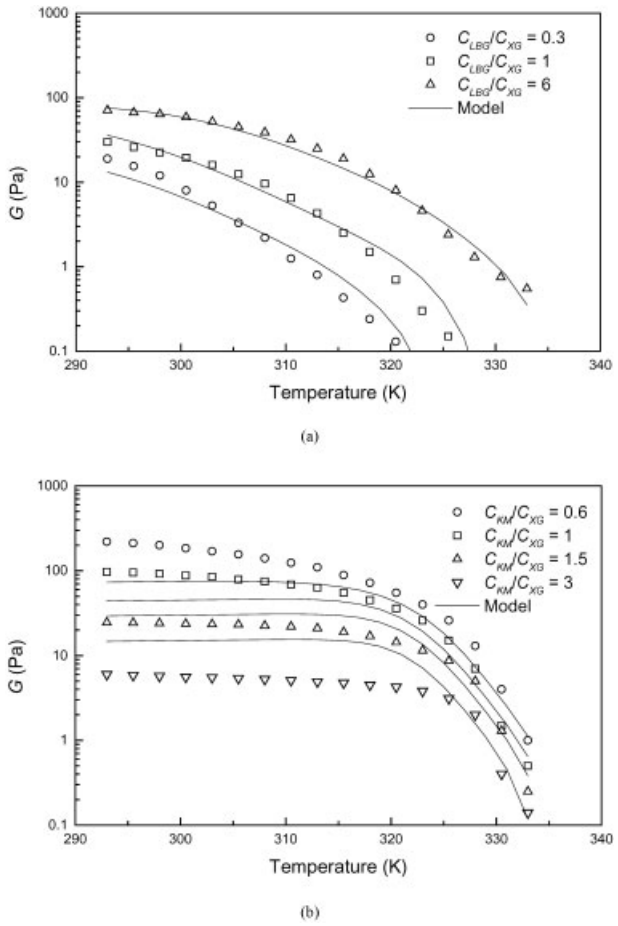

Figure 6 Testing of the temperature dependence of gel modulus using eq. (7) for two-component gels (data from Goycoolea et al.[24]). (a) 0.1% (w/v) deacetylated xanthan mixing with different concentrations of locust bean gum; (b) 0.24% (w/v) konjac glucomannan mixing with different concentrations of deacetylated xanthan.

ature dependence of gel modulus for the galactomannan/xanthan system and the glucomannan/xanthan system at different concentration ratios. In our previous study,[8] we have analyzed the concentration dependence of gel modulus for these gels and have shown that the cascade model can be successfully applied to describe these data. In this study, the temperature dependence data are analyzed using the aforementioned temperature dependence equations.

Figure 6 shows the rheological cooling data reported by Goycoolea et al.[24] for locust bean gum (LBG)/deacetylated xanthan (XG) mixed gels and konjac glucomannan (KM)/XG mixed gels at different concentration ratios. It is noted that the total polymer concentration in the data of Goycoolea et al. is not fixed. Therefore, the gel modulus variation with respect to changes in the composition may be simply due to changes in the total polymer concentration. Nevertheless, the gel modulus for both mixed gels shows strong temperature dependence, similar to that predicted by the cascade model.

To obtain the parameters of the cascade model, a nonlinear least-squares computer program is developed to curve fit the experimental data in Figure 6 using eq. (7). The Levenberg–Marquardt algorithm[25] was utilized in this program to optimize the parameters a, $\Delta H°$, and ΔS ° at fixed values of f_A and f_B by minimizing the object function:

$$\chi^2 = \sum(\ln G_i^{\exp} - \ln G_i^{\mathrm{mod}})^2 \qquad (8)$$

The other two parameters, f_A and f_B, because of their discrete nature, have to be found using a direct search method. Thus, executing the program generates a table of minimized χ^2 for a discrete set of f_A and f_B. Furthermore, it is assumed that the molecular weight of each polymer is 10^6. All the data sets with different compositions are fitted simultaneously by the program, and to reduce the regression time, only a subset of data points is used.

The optimized value of the object function for each system as a function of component functionality is shown in Figure 7. It can be seen that the minimum of the object function occurs at high functionalities. The cascade parameters at high functionalities are thus given here and discussed in detail for each system.

Table I lists the fitting parameters of the cascade equation at some sets of high functionalities for LBG/XG mixed gels. It is evident that χ^2 has a minimum around $f_{XG} = 300$. On the other hand, the best value of f_{LBG} cannot be determined without ambiguity, since χ^2 values are almost identical for f_{LBG} greater than 300. If the parameter set of $f_{LBG} = 500$ and $f_{XG} = 300$ is used in the cascade model, it can be found that the resulting curves (solid curve in Fig. 6(a)) agree excellently with the experimental data. Two features of the parameter set of $f_{LBG} = 500$ and $f_{XG} = 300$ should be noted. First, the dimensionless enthalpy–entropy ratio has a value of 1.15, which does not obey eq. (6). Second, the value of front factor is much less than unity.

In addition to the above features, two questions arise regarding these high functionalities. First, the best-fit parameters are in disagreement with those obtained from the concentration dependence of gel modulus.[8] For example, the values of functionality ($f_{LBG} = 500$ and $f_{XG} = 300$) are much higher than those obtained from the concentration dependence data ($f_{LBG} = 30$ and $f_{XG} = 50$). Second, these high functionalities do not seem to be compatible with the polymer structure. LBG is a galactomannan consisting of a manann backbone branched with galactose units with a mannose to galactose ratio of approximately 4:1.[26] Dea et al.[27] have proposed that the interaction of LBG with other polysaccharides occurs in the LBG segment with more than six consecutive galactose-free mannose units. In comparison with the theoretical distri-

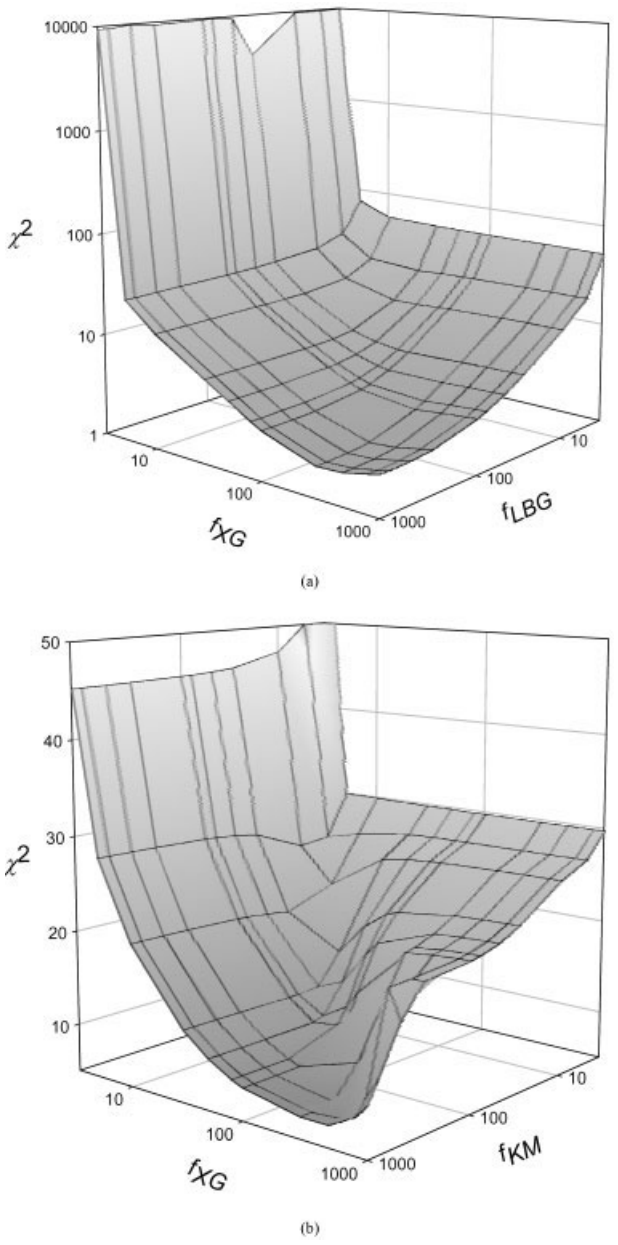

Figure 7 The object function χ^2 as a function of functionalities obtained by fitting the data of Figure 6 using eq. (7). (a) LBG/XG mixed gels; (b) KM/XG mixed gels.

bution of galactose-free mannan segments,[28] the value of $f_{LBG} = 500$ is comparable to that with more than three consecutive galactose-free mannose units, which is much larger than that obtained according to the model described by Dea et al. On the other hand, the value of $f_{XG} = 300$ corresponds to a ratio of one functional group for every three repeating units (the repeating unit of XG consisting of five sugar residues and substituents[29]) along the polymer main chain. This ratio seems impractically high. These two inconsistencies suggest that the functionalities obtained from the rheological cooling data for LBG/XG mixed gels may be overestimated. A possible explanation for the high functionalities is that the rheological gelling process may involve mechanisms other than the association between component polymers, such as a structural rearrangement (see below for KM/XG mixed gels), which is not included in the cascade model.

TABLE I
Fitting Parameters of the Cascade Equation for LBG/XG Mixed Gels

f_{LBG}	f_{XG}	a	$-\Delta H°$ (kJ/mol)	$-\Delta S°$ (kJ/(K mol))	χ^2
1000	300	0.111	123	0.361	2.00
800	300	0.114	123	0.358	2.00
500	300	0.113	124	0.358	2.04
300	300	0.120	124	0.354	2.14
1000	800	0.075	127	0.382	2.32
1000	500	0.091	125	0.371	2.06
1000	100	0.185	118	0.336	3.01

For KM/XG mixed gels, some of the best-fit parameter values are listed in Table II. It can be seen that χ^2 has a minimum value around $f_{KM} = 1000$, whereas the χ^2 values are almost identical at $f_{XG} = 300$ and 500. If the parameter set of $f_{KM} = 1000$ and $f_{XG} = 300$ is used in the cascade model, the resulting curves [solid curves in Fig. 6(b)] agree fairly with the experimental data. It is noted that the deviation between the model curves and data points becomes significant at low temperatures.

Again, the high functionalities seem to be questionable on a molecular basis. To evaluate the validity of the model parameters, a heat output profile as a function of temperature is generated using the cascade model and compared with an experimental differential scanning calorimetry (DSC) thermogram. Figure 8 displays the experimental cooling thermogram reported by Goycoolea et al.[24] and the calculated heat output based on the parameter set of $f_{KM} = 1000$ and $f_{XG} = 300$. The DSC thermogram has a peak temperature of ε330 K, higher than that obtained from the cascade model, followed by a slight shoulder at lower temperatures. It is noted that the position of the shoulder is roughly coincident with the calculated peak

TABLE II
Fitting Parameters of the Cascade Equation for KM/XG Mixed Gels

f_{KM}	f_{XG}	a	$-\Delta H°$ (kJ/mol)	$-\Delta S°$ (kJ/(K mol))	χ^2	$-\Delta H$ (J/g XG)
1000	300	0.025	350	1.03	7.23	105
800	300	0.025	354	1.05	7.26	106
500	300	0.025	366	1.08	7.44	110
300	300	0.029	351	1.03	10.4	105
1000	800	0.010	388	1.15	8.75	310
1000	500	0.015	376	1.11	7.21	118
1000	100	0.071	286	0.84	8.37	29

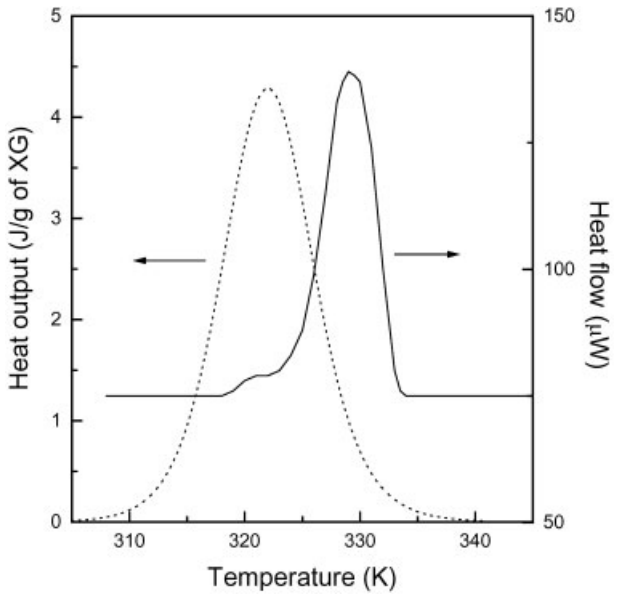

Figure 8 Comparison of the heat flow obtained from the DSC cooling scan (data from Goycoolea et al.[24]) and the heat output derived using the cascade model for KM/XG mixed gels (0.2% (w/v) konjac glucomannan mixing with 0.1% (w/v) deacetylated xanthan). Solid curve, the DSC cooling scan; dotted curve, the heat release curve generated using the parameters $f_{KM} = 1000$, $f_{XG} = 300$, $-\Delta H° = 350$ kJ/mol, and $-\Delta S° = 1.03$ kJ/(K mol).

temperature. The difference between these two curves is apparent.

An interpretation of the DSC thermogram is that the major peak is associated with the formation of crosslinks between KM and XG, while the shoulder is associated with a structural rearrangement. A comparison of Figures 6(b) and 8 suggests that the buildup of elasticity primarily occurs during the structural rearrangement period, rather than the crosslink formation period. Since the current cascade model deals only with the crosslinking process, the resulting cascade parameters may be misleading. Moreover, the presence of a significant structural rearrangement leads to a large χ^2 value when compared with that for the LBG/XG mixed gel.

Another discrepancy is the enthalpy of gelation ΔH. A ΔH value of approximately -30 J/g of XG was obtained (Figure 8) by Goycoolea et al.,[24] whereas the parameter set of $f_{KM} = 1000$ and $f_{XG} = 300$ results in a ΔH value of –105 J/g of XG, 3.5 times higher than the experimental value. Interestingly, the parameter set of $f_{KM} = 1000$ and $f_{XG} = 100$ yields a ΔH value of –29 J/g of XG, comparable to the experimental value. It appears that in terms of thermal behavior, the parameter set of $f_{KM} = 1000$ and $f_{XG} = 100$ gives the best result (see Table II).

For the LBG/XG mixed gel, unfortunately, the DSC thermogram is featureless and no comparison can be made. However, it is reasonable to assume that a minor structural rearrangement may exist for the LBG/XG mixed gel during cooling, since gels are formed with similar interaction patterns for both systems. This may explain the unusual model parameters discussed previously.

It can be concluded that the cascade model can be used to approximate the rheological gelling data for LBG/XG mixed gels and KM/XG mixed gels. However, care must be taken in interpreting the physical meaning of the model parameters, especially when the thermal process involves a mechanism other than the association between component polymers.

SOL–GEL PHASE DIAGRAM

For a thermoreversible gel, it undergoes a sol–gel transition at elevated temperatures. The concentration dependence of the melting temperature T_m for a single-component thermoreversible gel can be described by the Eldridge–Ferry equation[10]:

$$\frac{\partial \ln C}{\partial (1/T_m)} = \frac{\Delta H_m}{R} \tag{9}$$

where ΔH_m represents the melting enthalpy of crosslinks. The value of ΔH_m can be obtained from a plot of ln C versus $1/T_m$.

In the cascade model, when the temperature dependence of the equilibrium constant is assumed to follow the van't Hoff-type relation, the critical condition can be reduced to the Eldridge–Ferry equation. This can be shown as follows. Taking the derivative of eq. (3) with respect to temperature leads to the van't Hoff equation:

$$\frac{\partial \ln K}{\partial T} = \frac{\Delta H^o}{RT^2} \text{ or } \frac{\partial \ln K}{\partial (1/T)} = -\frac{\Delta H^o}{R} \tag{10}$$

At the critical point (sol–gel transition), the equilibrium constant is related to the critical concentration by the following expression[8]:

$$K = \frac{M(f-1)}{Cf(f-2)^2} \tag{11}$$

Since M and f are temperature-independent, the derivative of ln K with respect to temperature is thus equal to the minus derivative of ln C:

$$\frac{\partial \ln K}{\partial T} = -\frac{\partial \ln C}{\partial T} \tag{12}$$

Inserting eq. (12) into eq. (10) yields the Eldridge–Ferry expression, in which $\Delta H°$ is set to be equal to ΔH_m.

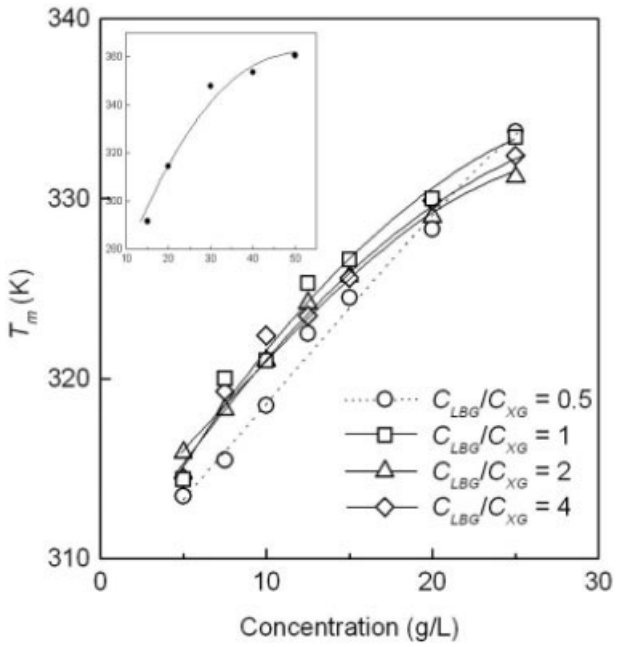

Figure 9 Dependence of T_m on concentration for LBG/XG mixed gels at different concentration ratios. The inset shows T_m versus concentration data for XG gels.

For a two-component thermoreversible gel, the equilibrium constant is also inversely proportional to the critical concentration[8]:

$$K = \frac{(1+r)\alpha_{A0}M_B}{rCf_B(1-\alpha_{A0})(1-\alpha_{B0})} \tag{13}$$

where α_{A0} and α_{B0} represent the critical conversions. Since α_{A0} and α_{B0} are also temperature-independent, eq. (12) is still valid, and the Eldridge–Ferry equation can be used without modification to model the sol–gel transition of a two-component thermoreversible gel.

In what follows, the LBG/XG mixed gel is re-examined to demonstrate the applicability of the Eldridge–Ferry equation to two-component systems. The mixed gel was prepared via mixing LBG (Sigma, St. Louis, MO) and XG (Aldrich, Milwaukee, MI) at room temperature in deionized water and then heating to 85°C for 30 min. A mannose/galactose ratio of 3.28 for LBG was determined by the alditol acetate method.[30] The molecular weights of LBG and XG are 1.69×10^6 and 9.80×10^5, respectively, estimated from the Mark–Houwink equation.[31,32] The melting temperature for the mixed gel of a fixed concentration ratio was determined by the "test tube upside-down" method[33] at different polymer concentrations. The test tube was immersed in a water bath, where the temperature was allowed to rise at a rate of 1 K/min approximately.

Figure 9 shows the sol–gel phase diagram of LBG/XG mixed gels at different concentration ratios. The gel melting point increases with increasing polymer concentration, a behavior typical of a thermoreversible gel. It can be seen that the change in concentration ratio does not significantly affect the concentration dependence of T_m. At low $C_{\mathrm{LBG}}/C_{\mathrm{XG}}$ ratio, T_m becomes slightly more concentration-dependent (a higher slope of the sol–gel curve). Since it has been demonstrated in the previous study[8] that the weak gel behavior of XG becomes significant at high XG content, the sol–gel phase diagram of XG weak gels was also determined, as shown in the inset of Figure 9. The sol–gel curve of XG gels is different from those of LBG/XG mixed gels in two ways: the curve is more concentration-dependent, and the formation of XG gels requires higher polymer concentrations. The effect of aging was evaluated by allowing some gels to age at room temperature for a week. The resulting gel melting points were almost unchanged. Thus, the equilibrium assumption in the Eldridge–Ferry equation is satisfied.

To test the applicability of the Eldridge–Ferry equation to two-component thermoreversible gels, the data in Figure 9 are replotted in terms of ln C versus $1000/T_m$ in Figure 10. The Eldridge–Ferry plot shows a fairly linear relationship and the melting enthalpy can be calculated from the slope of the plot. The resulting values of ΔH_m are listed in Table III. It can be seen that at high $C_{\mathrm{LBG}}/C_{\mathrm{XG}}$ ratio the Eldridge–Ferry plots almost overlap each other and give a ΔH_m value of approximately -80 kJ/mol. The slope of the plot becomes less steep at low $C_{\mathrm{LBG}}/C_{\mathrm{XG}}$ ratio, thus leading to a less negative ΔH_m; for example, at $C_{\mathrm{LBG}}/C_{\mathrm{XG}}$

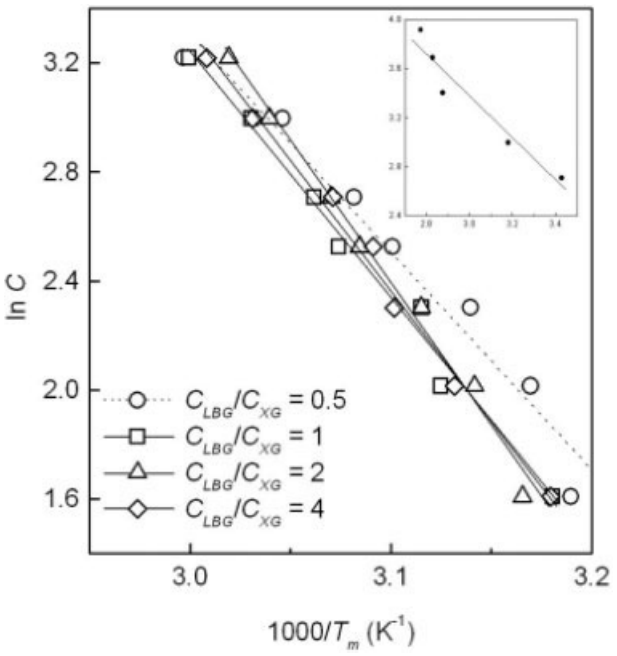

Figure 10 Eldridge–Ferry plots for LBG/XG mixed gels at different concentration ratios. The inset shows the Eldridge–Ferry plot for XG gels.

TABLE III
Melting Enthalpies for LBG/XG Mixed Gels and XG Gels

Sample	C_{LBG}/C_{XG}	$-\Delta H_m$ (kJ/mol)
LBG/XG	4	80
LBG/XG	2	87
LBG/XG	1	75
LBG/XG	0.5	67
XG	0	14

= 0.5, ΔH_m has a value of −67 kJ/mol. As for XG gels, the slope becomes much flatter, having a ΔH_m value of −14 kJ/mol.

It is noted that the magnitude of ΔH_m obtained from the sol–gel phase diagram is somewhat lower than the that of $\Delta H°$ estimated from the G versus T curves. This difference may be due to two reasons. First, the rheological gelling curve may be complicated by a structural rearrangement. Thus, the $\Delta H°$ value does not reflect the enthalpy change of the association between component polymers. Second, since the gel modulus is measured according to the ability of a gel to restore its original dimensions, whereas the "test tube upside-down" method is developed based on the ability of a gel to support its own weight under gravity, the gel network probed by these two methods may not be the same.

Another issue is that the derivation of eq. (9) from the cascade model implies that the enthalpy change is concentration-ratio independent. However, the plot of ΔH_m as a function of concentration ratio, as shown in Figure 11, indicates that the assumption of concentration-ratio independence is probably valid at high C_{LBG}/C_{XG} ratio, but fails at low C_{LBG}/C_{XG} ratio, where the magnitude of ΔH_m seems to drop toward the limiting value at $C_{LBG}/C_{XG} = 0$ (XG weak gels). The change in ΔH_m is certainly due to the gradual domination of network junctions by the self-association of XG at low C_{LBG}/C_{XG} ratio. However, the current model does not include the self-association of XG, and eq. (9) is derived based on a single reaction scheme. For these reasons, ΔH_m obtained from the Eldridge–Ferry plot must be considered as a semiempirical parameter, which depends on the effect of the self-association of XG. At the two extremes, the physical meaning of ΔH_m is clear: at $C_{LBG}/C_{XG} = 0$, ΔH_m represents the melting enthalpy for XG gels, and at $C_{LBG}/C_{XG} \rightarrow \infty$, ΔH_m is simply related to the association between LBG and XG. The decrease in magnitude of ΔH_m between the two extremes indicates that the contribution of the self-association of XG on the gel network becomes increasingly significant.

CONCLUSIONS

The temperature dependence of gel properties of two-component physical gels can be described by a simple cascade model. It is assumed that the temperature dependence of the equilibrium constant for the association between component polymers follows the van't Hoff-type relation. Since conversions and extinction probabilities, which determine the network structure, can be calculated with the knowledge of the equilibrium constant, the temperature dependence of a gel network as well as its elasticity can be estimated. It is found that the G versus T curve is strongly affected by the values of $\Delta H°$ and $\Delta S°$ such that the system may be thermoreversible or thermoirreversible. For thermoreversible mixed gels, the solution of the cascade equation under critical conditions combined with the van't Hoff equation can be reduced to the Eldridge–Ferry equation. It is also demonstrated that the Eldridge–Ferry equation can be used to model the sol–gel phase diagram of a two-component thermoreversible gel.

The rheological gelling data for galactomannan/xanthan and glucomannan/xanthan mixed gels were used to demonstrate the applicability of the cascade model. The parameters of the cascade model were obtained from the experimental data using a nonlinear curve fitting method. Though the resulting model curves agree fairly with the experimental data, the physical meaning of these parameters is questionable. The major problem encountered in justifying the values of the model parameters for the two systems is that the gelling process may involve a structural rearrangement, which probably determines the gel modulus of both mixed gels. However, since the detailed mechanism of the structural rearrangement is not clear yet, it is not feasible to incorporate it into the model.

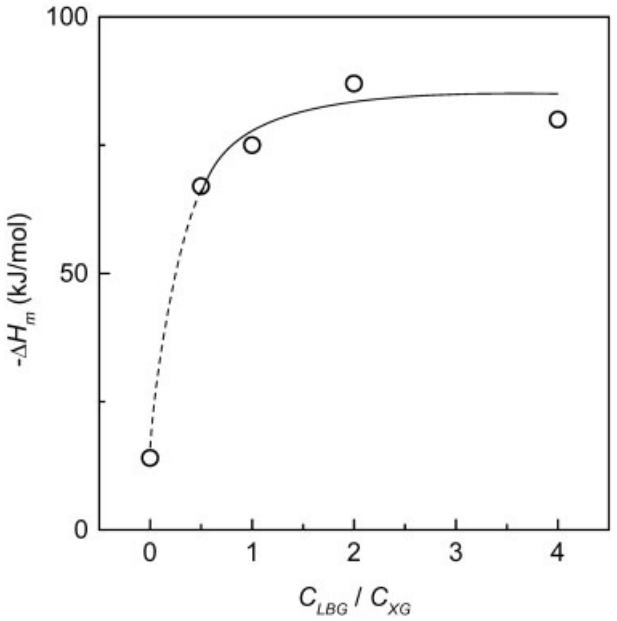

Figure 11 Dependence of the melting enthalpy of LBG/XG mixed gels on concentration ratio.

Despite this problem, it is concluded that the cascade model can be used to approximate the temperature dependence of the gel modulus of a two-component physical gel. The Eldridge–Ferry equation is also successful in modeling the sol–gel behavior of a two-component thermoreversible gel. Nevertheless, care must be taken in interpreting the results. A comparison with the cascade analysis of concentration dependence data is recommended. To justify the resulting parameters, it is also recommended to perform an auxiliary experiment, such as a calorimetric experiment.

References

1. Dea, I. C. M.; Morris, E. R.; Rees, D. A.; Welsh, E. J.; Barnes, H. A.; Price, J. Carbohydr Res 1977, 57, 249.
2. McCleary, B. V.; Dea, I. C. M.; Windust, J.; Cooke, D. Carbohydr Polym 1984, 4, 253.
3. Wolf, C. L.; Beach, S.; La Velle, W. M.; Clark, R. C. U.S. Pat. 4,876,105 (1989).
4. Papageorgiou, M.; Kasapis, S.; Richardson, R. K. Food Hydrocolloids 1994, 8, 97.
5. Lin, H. R.; Sung, K. C.; Vong, W. J. Biomacromolecules 2004, 5, 2358.
6. Kumar, S.; Himmelstein, K. J. J Pharm Sci 1995, 84, 344.
7. Morris, V. J. In Gums and Stabilisers for the Food Industry 3; Philips, G. O.; Wedlock, D. J.; Williams, P. A., Eds.; Elsevier: London, 1985.
8. Mao, C. F.; Chen, J. C. J Appl Polym Sci, 2006, 99, 2771.
9. Dobson, G. R.; Gordon, M. J Chem Phys 1965, 43, 705.
10. Eldridge, J. E.; Ferry, J. D. J Phys Chem 1954, 58, 992.
11. Richardson, P. H.; Clark, A. H.; Russell, A. L.; Aymard, P.; Norton, I. T. Macromolecules 1999, 32, 1519.
12. Bot, A.; Smorenburg, H. E.; Vreeker, R.; Pâques, M.; Clark, A. H. Carbohydr Polym 2001, 45, 363.
13. Clark, A. H.; Evans, K. T.; Farrer, D. B. Int J Biol Macromol 1994, 16, 125.
14. Scanlan, J. J Polym Sci 1960, 43, 397.
15. Case, L. C. J Polym Sci 1960, 45, 501.
16. Watase, M.; Nishinari, K. Polym J 1986, 18, 1017.
17. Tan, H. M.; Moet, A.; Hiltner, A.; Baer, E. Macromolecules 1983, 16, 28.
18. Mao, C. F.; Chen, C. H. J Appl Polym Sci 2003, 90, 4000.
19. Searle, M. S.; Westwell, M. S.; Williams, D. H. J Chem Soc Perkin Trans 2 1995, 141.
20. Ross-Murphy, S. B. Polymer 1992, 33, 2622.
21. Cairns, P.; Miles, M. J.; Morris, V. J. Nature 1986, 322, 89.
22. Copetti, G.; Grassi, M.; Lapasin, R.; Pricl, S. Glycoconjugate J 1997, 14, 951.
23. Cairns, P.; Miles, M. J.; Morris, V. J.; Brownsey, G. J. Carbohydr Res 1987, 160, 411.
24. Goycoolea, F. M.; Richardson, R. K.; Morris, E. R.; Gidley, M. J. Macromolecules 1995, 28, 8308.
25. Marquardt, D. W. J Soc Ind Appl Math 1963, 11, 431.
26. Dea, I. C. M.; Morrison, A. Adv Carbohydr Chem Biochem 1975, 31, 241.
27. Dea, I. C. M.; Clark, A. H.; McCleary, B. V. Carbohydr Res 1986, 147, 275.
28. McCleary, B. V.; Clark, A. H.; Dea, I. C. M.; Rees, D. A. Carbohydr Res 1985, 139, 237.
29. Jansson, P. E.; Kenne, L.; Lindverg, B. Carbohydr Res 1975, 45, 275.
30. Blakeney, A. B.; Harris, P. J.; Henry, R. J.; Stone, B. A. Carbohydr Res 1983, 113, 291.
31. Gaisford, S. E.; Harding, S. E.; Mitchell, J. R.; Bradley, T. D. Carbohydr Polym 1986, 6, 423.
32. Torres, L. G.; Brito, E.; Galindo, E.; Choplin, L. J Ferment Bioeng 1993, 75, 58.
33. Hong, P. D.; Chen, J. H. Polymer 1998, 39, 711.